

Optimization of a new liquid scintillation spectrometer for the measurement of environmental levels of ^3H in water samples

J.L. García-León^{a,*}, M. García-León^b, G. Manjón^a, J. Rivera-Silva^c

^a Universidad de Sevilla. Departamento de Física Aplicada II, Escuela Técnica Superior de Arquitectura, Av. Reina Mercedes 2, 41012, Sevilla, Spain

^b Universidad de Sevilla. Departamento de Física Atómica, Molecular y Nuclear, Facultad de Física, Av. Reina Mercedes s/n, 41012, Sevilla, Spain

^c Servicio de Radioisótopos, Centro de Investigación, Tecnología e Innovación (CITIUS), Universidad de Sevilla, Av. Reina Mercedes 4B, 41012, Sevilla, Spain

ARTICLE INFO

Handling Editor: Sheldon Landsberger

ABSTRACT

The activity concentration of ^3H in water samples collected from places unaffected by nuclear activities or for human consumption can be very low. In these cases, determination procedures must achieve a Minimum Detectable Activity (MDA) low enough to ensure that ^3H is accurately determined. In this paper, we present a method that uses a new Liquid Scintillation Spectrometer (LSC in what follows): the Quantulus GCT 6220. Furthermore, a new liquid scintillation cocktail, the ProSafe LT+, has been tested for ^3H measurement, showing to be a good option for the determination of low levels of this radionuclide. The MDAs achieved are low enough to enable the measurement of very low levels of ^3H in recent environmental water. The results obtained using a Quantulus GCT 6220 and Prosafe LT+ are compared to those obtained with a Quantulus 1220 and Prosafe HC+ as liquid scintillation cocktail.

1. Introduction

^3H is a radioactive isotope of hydrogen with a half-life of 12.32 ± 0.02 years, and decays by β^- emission with a maximum energy of 18.5906 ± 0.0032 keV (Purcell and Sheu, 2015). Such low energy makes LSC our technique of choice for its determination in environmental samples.

^3H is present in the environment due to different natural and artificial sources. The natural production of ^3H comes from the interaction of cosmic rays with stable ^{14}N in the upper atmosphere: ($^{14}\text{N} + n \rightarrow ^{12}\text{C} + ^3\text{H}$) (P. G. Young and Foster, 1972). ^3H can also be found in neighbouring waters of nuclear power plants [3], ^3H production facilities, and nuclear test sites (Oms et al., 2019). Other sources include nuclear accidents (Machida et al., 2023; Povinec et al., 2017) and nuclear fuel reprocessing plants (Sudprasert et al., 2022) This artificial production of ^3H is expected to increase due to the future operation of nuclear fusion reactors where it will be used as fuel (Abdou et al., 2015).

The wide availability and high environmental mobility of ^3H (Ferreira et al., 2023; Oms et al., 2019) makes this radionuclide particularly relevant in monitoring programmes (Janković et al., 2012; La Verde et al., 2021; Sudprasert et al., 2022) where its determination in tap water is mandatory in many cases. One of such programmes is the

Spanish Environmental Radiological Surveillance Network, coordinated by the Spanish Nuclear Safety Council (Butragueño et al., 1992). Our laboratory belongs to such network and, therefore, is committed to the measurement of ^3H in tap water.

The activity concentration of ^3H in tap water samples from the city of Seville (Spain) has been decreasing during the last years. An example can be seen in Fig. 1 where data on the concentration of ^3H in tap water collected in Seville are presented together with the systematic Minimum Detectable Activities (MDA) so far obtained with the previous methods used at our laboratory. In recent years, the activity concentrations have been too close to MDA. We expect that the cause of this decrease might be the global decay of tritium, as there has been no significant contribution from nuclear tests in the last three decades and there are no nuclear power plants in the vicinity of the city of Seville. A similar decay has been observed in several areas (Duliu et al., 2018; Gusyev et al., 2016). This makes it necessary to achieve an improvement in our procedure to lower the MDA to allow a realistic determination of ^3H concentration in human consumption water.

An increase of MDA can be seen at some points in Fig. 1. The counting efficiency and background count rate proved to be stable at that time in our Quantulus 1220 spectrometer, these sharp changes are due to the electrolytic enrichment: The concentration factor was an

* Corresponding author. Universidad de Sevilla. Departamento de Física Aplicada II, Escuela Superior de Arquitectura, Av. Reina Mercedes 2, 41012, Sevilla, Spain.
E-mail address: jgarcia34@us.es (J.L. García-León).

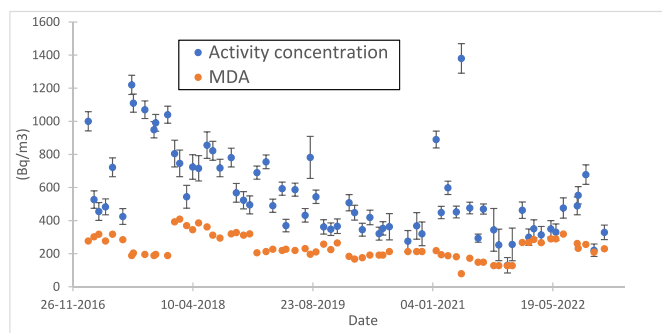


Fig. 1. ^3H activity concentration in drinking water results and MDAs obtained in Seville from January of 2017 to December of 2022 [12]. A steady decrease in activity concentration can be contemplated.

average of 4.55 for all 12 samples, while it was 6.48 in 2019. Some possible explanations for this could be a poor refrigeration of the system in 2018 or cells that weren't properly cleaned.

Our previous measurement technique was based on the use of a Quantulus 1220 LSC and ProSafe HC + as a liquid scintillation cocktail. Although the mentioned spectrometer is designed for low-level counting, under current conditions, our present method does not provide a low enough MDA. To overcome this problem, we have carried out a set of improvements of the procedure aimed to decreasing the MDA to make it possible to determine ^3H at the very low levels recently found in drinking water.

After a new measurement procedure with a lower MDA was established, it was validated by measuring a proficiency test sample that served as quality control. After confirming that the results are valid and reliable, this method was used for the determination of ^3H in tap water samples for monitoring.

2. Experimental

Tap water samples from the public water supply in Seville were collected monthly from 2016 to 2023. After sampling, they were stored until analysis. The procedure is applied to six samples simultaneously. Our first step was to purify and concentrate to make possible the measurement of ^3H by LSC. For this, water was first distilled. Then, 1.00 g of Na_2O_2 was added to each sample to increase the electrical conductivity. In routine tasks, our set of six samples was analysed along with one procedural blank and three additional spiked samples to determine the enrichment factor to a total of 10 concurrent analyses.

The second step was electrolysis (Baeza et al., 1999). Our choice is to concentrate each of the 10 samples from 250 ml to 20 ml in stainless steel electrolytic cells. A schematic of this electrolysis system is shown in Fig. 2. Finally, PbCl_2 is used to neutralise the final samples that are distilled once again. Additional spiked and blank vials were used for efficiency calibrations and background determinations, respectively. The ^3H spike solution was provided by the Physikalisch-Technische Bundesanstalt and had an activity concentration of 9.13 Bq/g on January 01, 2005.

Once this is done, two alternative methods have been used to continue the experimental procedure. Following the first method, the sample is mixed with the Prosafe HC + liquid scintillation cocktail in a scintillation vial and measured with a Quantulus 1220 spectrometer. In the second method, the sample is mixed with the ProSafe LT + scintillation cocktail inside a vial and measured with the Quantulus GCT 6220 spectrometer for ^3H determination. ^3H activity concentration and the corresponding MDA were evaluated according to the equations that are listed in a previous publication (Villa and Manjón, 2004). The scintillation vials used for this study were provided by Meridian Bio-technologies Ltd. They are made of polyethylene and allowed to measure a mixture of up to 20 ml, which corresponds to the total volume

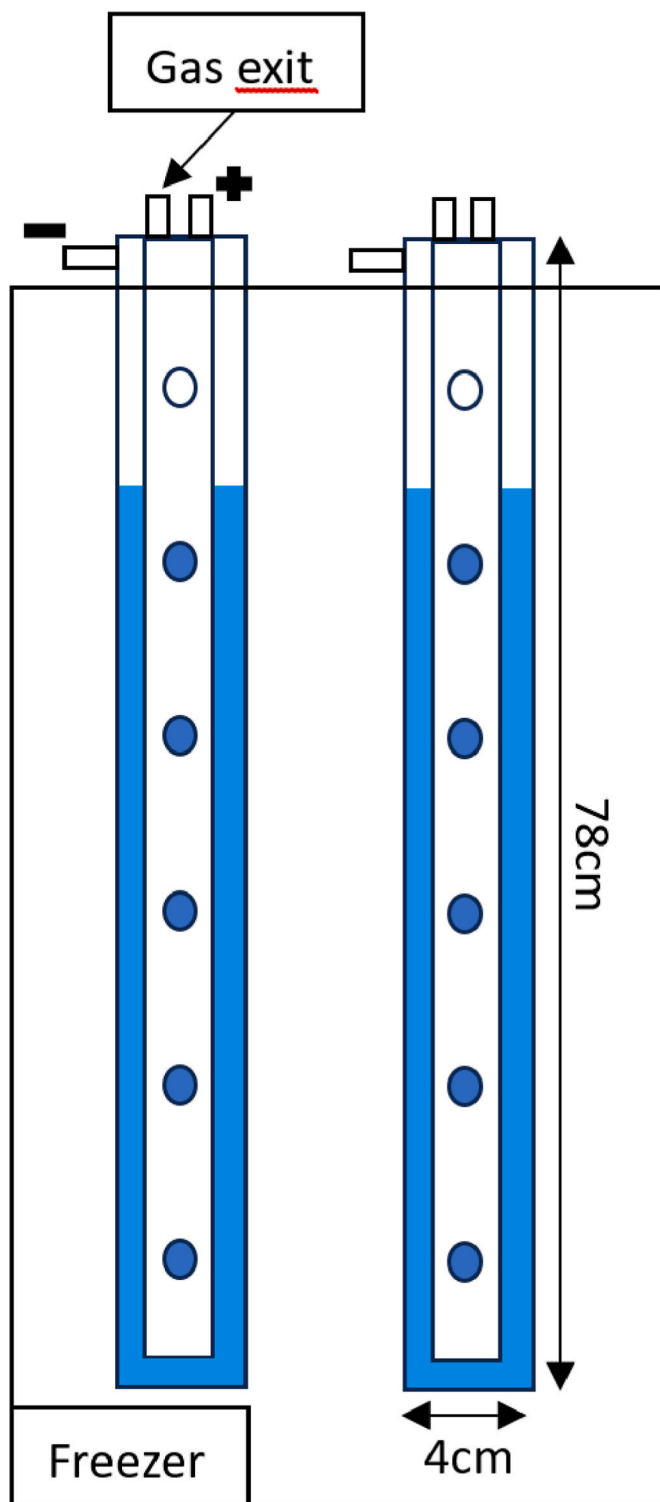


Fig. 2. Schematic of our electrolysis system. The outer shell of an electrolytic cell is connected to the negative terminal of a current source, while the inner rod to the positive terminal. A current will, consequently, flow through the water sample, starting an electrolytic process. A gas exit is used to conduct the H_2 and O_2 produced in the reaction outside of the laboratory. This entire process is performed inside a freezer to prevent the water from boiling, which would produce an important loss of tritium. All 10 electrolytic cells are connected in series to ensure that the same intensity runs through all of them.

introduced in each vial used for this study.

The activity concentration at the time of sampling was determined as follows.

$$A \left(\frac{\text{Bq}}{\text{L}} \right) = \frac{\Sigma_S - \Sigma_B}{\varepsilon \cdot V \cdot 60} e^{\frac{\ln 2 \cdot t_e}{T_{1/2}}} \cdot \frac{1}{\left(\frac{m_i}{m_f} \right)^{\bar{P}}} \quad [1]$$

Where Σ_S, Σ_B are the count rates (in counts per minute) of the sample and background respectively, ε is the counting efficiency, V the volume inside the counting vial (in liters), t_e the time elapsed between sample collection and the measurement, $T_{1/2}$ is the half-life of ^3H and m_i, m_f the sample masses before and after enrichment. \bar{P} is the enrichment parameter defined as (Villa and Manjón, 2004):

$$P_j = \frac{\ln \left(\frac{\Sigma_{\text{spiked},j} - \Sigma_B}{A_{\text{spiked},j} \cdot V_{\text{spiked},j} \cdot \varepsilon \cdot 60} \right)}{\ln \left(\frac{m_{\text{spiked},i,j}}{m_{\text{spiked},f,j}} \right)}, j = 1, 2, 3 \quad [2]$$

Where $\Sigma_{\text{spiked},j}$ is the count rate obtained for each one of the three spiked samples. $A_{\text{spiked},j}$ refers to the activity of the spike added to each cell, $V_{\text{spiked},j}$ is the volume of each spiked sample inside the vial after the procedure, and $m_{\text{spiked},i,j}, m_{\text{spiked},f,j}$ are the masses of the spiked samples before and after electrolysis. An enrichment parameter is obtained for each spiked sample. The three results are averaged for obtaining \bar{P} :

$$\bar{P} = \frac{\sum_{j=1}^3 P_j}{3} \quad [3]$$

Regarding the determination of MDA, it is done according to (Villa and Manjón, 2004; Currie, 1968):

$$\text{MDA} \left(\frac{\text{Bq}}{\text{L}} \right) = \frac{2.71 + 4.75 \sqrt{\Sigma_B \cdot t}}{\varepsilon \cdot V \cdot 60 \cdot t} \cdot \frac{1}{\left(\frac{m_i}{m_f} \right)^{\bar{P}}} \quad [4]$$

Where t (min) is the measurement time for the sample.

3. Results

3.1. Switching to ProSafe LT+ as a scintillation cocktail

Because MDA was close to the expected activity concentration, a change in the choice of scintillation cocktail was studied. The new liquid scintillation cocktail was ProSafe LT+ with the aim of decreasing the MDA of our technique without changing the sample preparation or counting time. The parameters used to compare both cocktails are presented in Table 1. A previous study on the response of this scintillation cocktail can be found in (Varlam et al., 2019), where several aspects of ProSafe LT+ are assessed as it is a competitive REACH-compliant solution for the determination of ^3H . Our results show good agreement with those obtained by the authors.

Table 1

Measured values of the parameters affecting the minimum detectable activity and minimum detectable activity using two different liquid scintillation cocktails. These results were obtained by measuring spiked and blank vials in a Quantulus 1220 LSC.

Parameter	ProSafe HC+ (Jan–Apr, 2022)	ProSafe LT+ (Sept–Oct 2022)
Efficiency (%)	24.3 ± 2.1	24.6 ± 3.5
Background (cpm)	1.1 ± 0.5	0.61 ± 0.03
Sample volume (ml)	5	8
MDA (Average) (Bq/m ³)	394	226

In Table 1 we can see that the MDA is reduced by using this new scintillation cocktail. This is mainly due to the reduction in the background count rate in the ^3H region (From 1.1 cpm with the ProSafe HC+ cocktail to 0.61 cpm with ProSafe LT+), see Fig. 3, and to the fact that this new cocktail has a higher capacity for neutral (pH = 7) samples. This allows the introduction of a sample volume up to 8 ml inside the vial, instead of the 5 ml previously used with the ProSafe HC+. These two factors reduce the MDA according to Eq. (4).

The background spectra obtained with our Quantulus 1220 for each scintillation cocktail are depicted in Fig. 3. There is a significant difference between the count rates in the low-energy region, which is specifically where the ^3H counts will appear. For ^3H measurements in the Quantulus 1220, the summing window including channels 28–154 was used.

3.2. Optimization of the quantulus GCT 6220

Although we achieved an improvement by switching to a different scintillation cocktail, our aim was to push the MDA to lower levels. A second measure taken for the decrease of the MDA was using a newer low background LSC, the Quantulus GCT 6220.

This new spectrometer can be used for low level determinations despite not having a thick passive shielding and separate Photomultiplier Tubes (PMTs) for guard detection. These shortcomings are compensated by using newer technology, which consists of a BGO (Bismuth Germanate, Bi₄Ge₃O₁₂) guard detector. Its light signal can be picked up by the coincidence PMTs and discriminated from the actual light pulses produced inside the vial. However, the BGO guard detector does not detect all background events. The GCT (Guard Compensation Technology) technology can be used to compensate for missed background events (Edler, 2017). This technique can be competitive with the more traditional thick shielding approach, but at the cost of making additional calibrations prior to each set of measurements.

Regarding this guard compensation, there is the GCT setting. A good discussion on the meaning of this parameter can be found in (Edler, 2017). In a measurement protocol, the GCT parameter can be set as OFF, LOW or HIGH. The background count rate decreases when the GCT parameter is changed from OFF to LOW or HIGH but counting efficiency should not be affected (Feng et al., 2017). The LOW and HIGH settings will optimize the guard efficiencies in different spectral regions: GCT LOW is better used in the region 0–112 keV, and GCT HIGH is used for

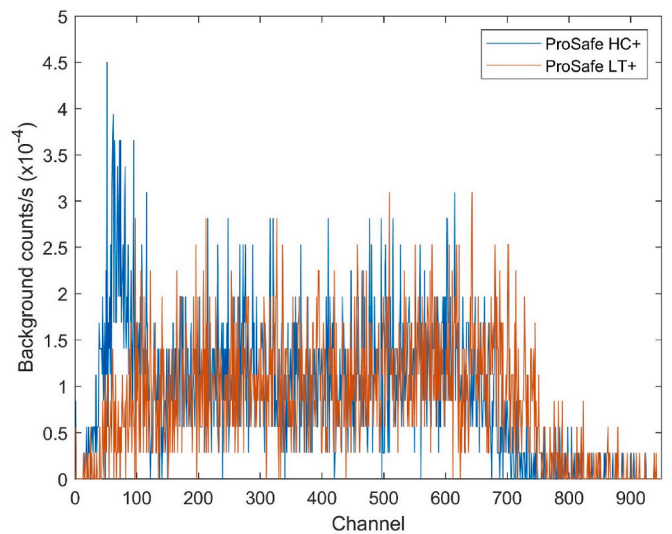


Fig. 3. Background spectra for each one of the scintillation cocktails. Backgrounds are similar for medium and high energies, but vastly different in the low energy region. This makes the background count rates fundamentally different for ^3H measurement applications.

counting in the region 0–28 keV (Edler, 2017). These efficiencies are automatically determined by the machine during routine calibrations.

To determine the impact of these settings on the measurement of ³H, they have been assessed and the corresponding efficiencies and background count rates calculated. The MDA was used as the optimization parameter due to the decrease in ³H levels in tap water collected in Seville. Results are shown in Table 2, where the GCT parameter was selected as OFF, LOW and HIGH. Background count rates were similar for OFF and LOW GCT settings, along with counting efficiency. The baseline MDA refers to that calculated with the efficiency and background count rate with all special measurement settings turned off and has a value of 284 Bq/m³.

Crosstalk correction was also evaluated, which works by using a Pulse Amplitude Comparison (PAC) circuit. Pulses with a height difference greater than a certain PAC parameter will be rejected, thus reducing crosstalk. This correction did not prove to reduce the MDA while GCT is in LOW setting for ³H measurements in our case. The luminescence correction setting was also evaluated, which works by performing single photon measurements. This allowed for a small reduction in MDA, but not enough for us to meet our objective. Finally, setting the GCT setting to HIGH allowed the background count rate to decrease from around 1 cpm–0.07 cpm, which allowed for an important reduction in the MDA.

For ³H measurements, the counting efficiency significantly decreased when GCT was set to HIGH. The MDA relative change listed in Table 2 has been defined in a way that allows to predict which combination will yield the lowest MDA in the analysis of real samples:

$$MDA_{rel} = \frac{\varepsilon_{OFF}}{\varepsilon_i} \frac{2.71 + 4.75\sqrt{\Sigma_{B,i} \cdot t}}{2.71 + 4.75\sqrt{\Sigma_{B,OFF} \cdot t}} \quad [5]$$

Being $\Sigma_{B,i}$ the background count rate for each row of Table 2, and ε_i the counting efficiency for that specific combination of settings. The sub-index 'OFF' refers to a measurement made with the GCT set to OFF.

According to our results, GCT HIGH must be set in the case of activity concentration levels close to the MDA. However, GCT OFF or GCT LOW could be a better selection for high activity concentration levels due to the higher counting efficiency. When setting the GCT to HIGH, some efficiency is lost, but the background count rate is greatly reduced.

3.3. Validation

The selected settings were validated by performing measurements of a Quality Control sample provided in the IAEA-TERC-2022-01/02 Proficiency Test. This was a water sample, which included ⁹⁰Sr, ²¹⁰Pb, ¹³⁷Cs, ¹³⁴Cs and ²⁴¹Am, along with ³H, in known amounts. Due to the presence of radionuclides other than ³H, this sample was double distilled before mixing with the scintillation cocktail ProSafe LT+. Three aliquots of this distilled sample were taken and then diluted with blank water to different activity concentration levels, mixed with our liquid scintillation cocktail, and then measured with our settings to validate our system. Results are shown in Fig. 4.

According to our results, shown in Fig. 4, the new measuring

Table 2

Results of the optimization for different combinations of settings in the new spectrometer Quantulus GCT 6220. These were obtained with a measurement time of 600 min and the scintillation cocktail ProSafe LT+.

Mode	Efficiency (%)	Background (cpm)	MDA relative change
GCT OFF	22.9 ± 2.1	1.06 ± 0.09	1 (Baseline)
GCT LOW	21.2 ± 1.9	0.99 ± 0.09	1.04
GCT LOW + crosstalk correction (high)	20.5 ± 2.1	0.88 ± 0.15	1.02
GCT LOW + luminescence correction	21.2 ± 2.0	0.76 ± 0.12	0.91
GCT HIGH	17.4 ± 1.6	0.07 ± 0.03	0.36

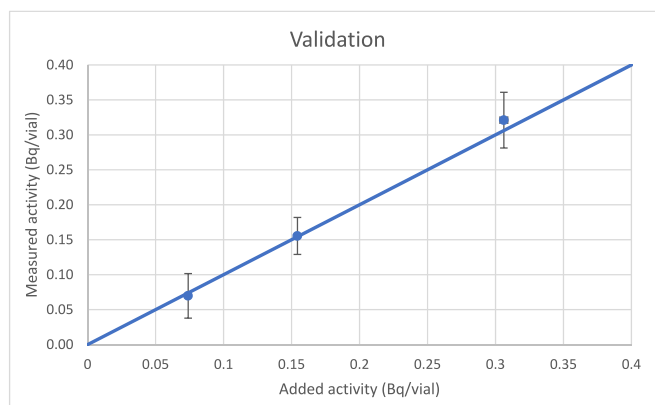


Fig. 4. Results of the validation procedure described previously. Measured activity is presented against added activity for each one of the three vials. The bisector shows that the measured activity is compatible with the nominal value.

procedure, consisting of the scintillation cocktail ProSafe LT+ and the use of the LSC Quantulus GCT 6220 is accurate. It is important to note that this only validates the measurement and not the electrolytic enrichment part of the process, as the Quality Control sample has not been concentrated by electrolysis. This was our choice because in this study, improvements were made only in the radiometric measurement, keeping the electrolytic enrichment the same as the last few decades.

3.4. Application to water samples

The new method based on the use of liquid scintillation cocktail Prosafe LT+ and the liquid scintillation spectrometer Quantulus GCT 6220) has made it possible to measure ³H in tap water collected in Seville for our monitoring work. This procedure has been used routinely from May to October of 2022 and during 2023 for monitoring measurements of ³H. Fig. 5 shows the valid monitoring results acquired with our improved technique. The MDAs obtained ranged from 74 Bq/m³ to 121 Bq/m³, which made possible the realistic measurement of environmental water samples, all of them with concentrations above MDA.

4. Conclusions

The use of ProSafe LT + has allowed for the determination of ³H with lower backgrounds and greater sample volumes inside the liquid scintillation vial, resulting in a decrease in MDA. This, along with the implementation and optimization of the newer liquid scintillation

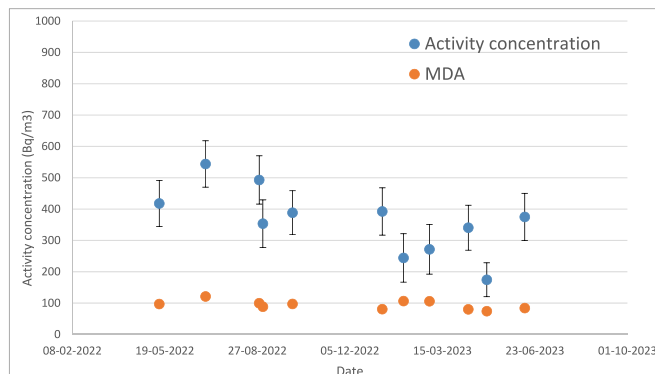


Fig. 5. Results of monitoring of ³H in drinking water in Seville using the optimized measurement procedure previously described: ProSafe LT+ and Quantulus GHT 6220 with GCT set to HIGH. Every data point is above the MDA, making the new method suitable for our scope of being capable of performing measurements of ³H in tap water reliably.

spectrometer Quantulus GCT 6220 has allowed us to continue making measurements of low activities of ^3H for monitoring work.

For the optimization of the Quantulus GCT 6220, different measurement modes, mostly based on the GCT parameter, have been compared. GCT HIGH has been the preferred option in the case of low activity concentrations of ^3H , and GCT OFF can be selected for high activity concentrations of ^3H . The results obtained using the new liquid scintillation cocktail and Quantulus GCT 6220 have been assured by comparing them to previous data. Additionally, the trueness of measurement has been confirmed using quality control samples.

CRedit authorship contribution statement

J.L. García-León: Conceptualization, Data curation, Formal analysis, Investigation, Methodology, Software, Visualization, Validation, Writing – original draft. **M. García-León:** Formal analysis, Funding acquisition, Project administration, Resources, Supervision, Writing – review & editing. **G. Manjón:** Formal analysis, Funding acquisition, Methodology, Project administration, Resources, Supervision, Writing – review & editing. **J. Rivera-Silva:** Methodology, Supervision.

Declaration of competing interest

The authors declare that they have no known competing financial interests or personal relationships that could have appeared to influence the work reported in this paper.

Data availability

Data will be made available on request.

Acknowledgements

This research has been partially funded by Consejo de Seguridad Nuclear, as well as from the Grant PID2022-140680NB-I00 funded by MCIN/AEI/10.13039/501100011033 and by the European Union is acknowledged. The help of Prof. R. García-Tenorio is deeply acknowledged.

References

- Abdou, M., Morley, N.B., Smolentsev, S., Ying, A., Malang, S., Rowcliffe, A., Ulrickson, M., 2015. Blanket/first wall challenges and required R&D on the pathway to DEMO. *Fusion Eng. Des.* <https://doi.org/10.1016/j.fusengdes.2015.07.021>.
- Baeza, A., Garcia, E., Miró, C., 1999. A procedure for the determination of very low activity levels of tritium in water samples. *J. Radioanal. Nucl. Chem.* 241, 93–100. <https://doi.org/10.1007/BF02347294>.
- Butragueño, J.L., Garcia, J.P., Gil, E., Granada, M.J., 1992. The Spanish environmental surveillance radiological network (REVIRA). In: *International Congress of the International Radiation Protection Association (IRPA8)*. Montreal, pp. 1729–1732.

- Currie, L.A., 1968. Limits for qualitative detection and quantitative determination. *Anal. Chem.* 586–593. <https://doi.org/10.1021/ac60259a007>.
- Duliu, O.G., Varlam, C., Shnawaw, M.D., 2018. 18 years of continuous observation of tritium and atmospheric precipitations in Ramnicu Valcea (Romania): a time series analysis. *J. Environ. Radioact.* 190–191, 105–110. <https://doi.org/10.1016/j.jenvrad.2018.05.011>.
- Eidler, R.H.W., 2017. Measurement of ^3H , gross α/β and ^{222}Rn in drinking water using the new Quantulus GCT 6220. *J. Radioanal. Nucl. Chem.* 314, 695–699. <https://doi.org/10.1007/s10967-017-5391-y>.
- Feng, X.G., Jiang, G.H., Huang, J.H., Du, J.Y., He, Q.G., Wang, J.C., Chen, J., Liu, X.G., 2017. A performance comparison of two kinds of liquid scintillation counters from PerkinElmer, Inc. *J. Radioanal. Nucl. Chem.* 314, 629–635. <https://doi.org/10.1007/s10967-017-5428-2>.
- Ferreira, M.F., Turner, A., Vernon, E.L., Grisolia, C., Lebaron-Jacobs, L., Malard, V., Jha, A.N., 2023. Tritium: its relevance, sources and impacts on non-human biota. *Sci. Total Environ.* 876 <https://doi.org/10.1016/j.scitotenv.2023.162816>.
- Gusyev, M.A., Stewart, M.K., Yamazaki, Y., Morgenstern, U., Kashiwaya, K., Nishihara, T., Kuribayashi, D., Sawano, H., Iwami, Y., 2016. Application of tritium in precipitation and baseflow in Japan: a case study of groundwater transit times and storage in Hokkaido watersheds. *Hydrol. Earth Syst. Sci.* 20, 1–16. <https://doi.org/10.5194/hess-2016-164>.
- Janković, M.M., Todorović, D.J., Todorović, N.A., Nikolov, J., 2012. Natural radionuclides in drinking waters in Serbia. *Appl. Radiat. Isot.* 70, 2703–2710. <https://doi.org/10.1016/j.apradiso.2012.08.013>.
- La Verde, G., Artioli, V., D'Avino, V., La Commara, M., Panico, M., Polichetti, S., Pugliese, M., 2021. Measurement of natural radionuclides in drinking water and risk assessment in a volcanic region of Italy, Campania. *Water (Switzerland)* 13. <https://doi.org/10.3390/w13223271>.
- Machida, M., Iwata, A., Yamada, S., Otosaka, S., Kobayashi, T., Funasaka, H., Morita, T., 2023. Estimation of temporal variation of tritium inventory discharged from the port of Fukushima Dai-ichi Nuclear Power Plant: analysis of the temporal variation and comparison with released tritium inventories from Japan and world major nuclear facilities. *J. Nucl. Sci. Technol.* 60, 258–276. <https://doi.org/10.1080/00223131.2022.2093800>.
- Oms, P.E., Bailly du Bois, P., Dumas, F., Lazure, P., Morillon, M., Voiseux, C., Le Corre, C., Cossonnet, C., Solier, L., Morin, P., 2019. Inventory and distribution of tritium in the oceans in 2016. *Sci. Total Environ.* 656, 1289–1303. <https://doi.org/10.1016/j.scitotenv.2018.11.448>.
- Povinec, P.P., Liang Wee Kwong, L., Kaizer, J., Molnár, M., Nies, H., Palcsu, L., Papp, L., Pham, M.K., Jean-Baptiste, P., 2017. Impact of the Fukushima accident on tritium, radiocarbon and radiocesium levels in seawater of the western North Pacific Ocean: a comparison with pre-Fukushima situation. *J. Environ. Radioact.* 166, 56–66. <https://doi.org/10.1016/j.jenvrad.2016.02.027>.
- Purcell, J.E., Sheu, C.G., 2015. Nuclear data sheets for $A = 3$. *Nucl. Data Sheets* 130, 1–20. <https://doi.org/10.1016/j.nds.2015.11.001>.
- Sudprasert, W., Phattanasub, A., Srimork, P., Imlae, S., Wongpaiboonsuk, P., Wongwechwin, P., 2022. Low-level tritium measurement in tap water in Bangkok area and annual dose estimation. *Environ Nat Resour J* 20, 455–464. <https://doi.org/10.32526/enrj/20/202200066>.
- Varlam, C., Vagner, I., Faurescu, D., 2019. Performance of nonylphenol-ethoxylates-free liquid scintillation cocktail for tritium determination in aqueous samples. *J. Radioanal. Nucl. Chem.* 322, 585–595. <https://doi.org/10.1007/s10967-019-06702-7>.
- Villa, M., Manjón, G., 2004. Low-level measurements of tritium in water. In: *Applied Radiation and Isotopes*, pp. 319–323. <https://doi.org/10.1016/j.apradiso.2004.03.027>.
- Young, P.G., Foster Jr., D.G., 1972. *An Evaluation of the Neutron and Gamma-Ray Production Cross Sections for Nitrogen Work Supported by the Defense Nuclear Agency*.